Researchers Journal of Science and Technology (REJOST)

Response of Magnetometer and GPS Data before two Strong Seismic events of 24th August, 2018 and 1st March, 2019 in Peru

Jewel Thomas[1], Joshua Fashae[2], Ndifreke Udosen[1]

Received: January 7, 2024 /Accepted: March 5, 2024

Abstract

Earthquakes (EQs) constitute serious natural environmental hazards threatening lives on earth and are capable of inducing large-scale disturbances in global ionospheric dynamics and related parameters.Presently, there is no doubt that multi-precursors analysis is a necessary step to better understand the mechanism before large earthquakes, however, the swiftness in response by the various devices has not been fully studied.In this study, we investigated the response of both the magnetometer and the Global Positioning System (GPS) - total electron content (TEC) data simultaneously from two strong seismic events that occurred on August 24, 2018 (M7.1) and March 1, 2019 (M7.0) in Peru to ascertain their responsiveness to these events. Both magnetometer and the Global Positioning System data were simultaneously acquired within the same period for each seismic event. Quiet and disturbed plots were generated and correlated for the respective equipment in each EQ. Interplanetary, solar and geomagnetic data were also downloaded during these periods for the different events. For the March 1st, 2019 EQ, the difference between quiet and disturbed solar quiet (sq) as obtained by the magnetometer ranged from 5 nT to 50 nT. The highest variations occurred on February 28 and March 4, 2019 while the least was recorded on March 6, 2019. Both sets of devices contemporaneously presented irregularities on February 26 and 27, 2019. However, with respect to the swiftness of response, the magnetometer responded in the morning (being swifter) between 7 and 11am while the GPS responded to the signals in the evening (17:00 hours). Also, the M7.1 August 24 2018 EQ, was investigated between August 17th and 30th. Findings revealed that only the magnetometer was able to respond to the signals on August 17th, 18th, 20th and 22nd, 2018 from this

EQ, whereas the GPS had no response. Hence, in both studied EQs with different time windows, the magnetometer was more sensitive (being swifter) than the GPS in responding to the signals from the seismic events.

✉ Jewel Thomas: jewelemem@gmail.com

[1] Geophysics Research Group, Physics Department, Akwa Ibom State University

[2] Physics Programme, Bowen University, Iwo Osun State

Keywords**:** Magnetometer; GPS; Peru; Earthquake; Response

1.0 Introduction

Ionospheric responses to seismic activities have been widely studied by Liu *et al*. (2004), Ibanga, *et al*. (2017) and Thomas *et al*. (2021, (2022), (2024**).** Earthquakes constitute a serious natural environmental hazard threatening lives on earth and are capable of inducing large-scale disturbances in global ionospheric dynamics and related parameters. Its preparation process institutes one of the day-to-day ionospheric variabilities that still pose a major challenge for researchers globally. This is due to the fact that the coupling between the anomalously generated electric field in the earthquake preparation zone at the ground surface and the one generated in the ionosphere causes the ion drift that led to the modification of the ionosphere formation. Most of this variability is given as a deviation from the mean or median value. Quantitative estimations of the ionospheric variability have been reported (Kim and Hagei, 1997; Forbes *et al*., 2000; Rishbeth and Mendillo 2001; Pulinets *et al*., 2003). The effect on the ionosphere from below is seen as the primary cause of the daily variance as demonstrated in the review of Pulinets (1998), who suggested the effects of seismic activity through the electromagnetic coupling with the ionosphere, which is one of the sources of the ionospheric variability. A detailed report on the physical mechanism and main morphological features of the ionospheric changeability associated with seismic activity is described (Pulinets and Boyarchuks, 2004).

An earthquake being a dynamic phenomenon can be predicted through some geophysical and geochemical disparities in lithosphere, atmosphere and ionosphere during its preparatory stage. These seismic LAIC (Lithospheric - Atmospheric - Ionospheric Coupling) perturbations are commonly interpreted as earthquake precursors. A lot has been reported on seismo-ionospheric and geomagnetic responses before, during and after earthquakes from seismic LAIC anomalies (Parrot, 1995; Hayakawa and Molchanov, 2002; Pulinets and Boyarchuk, 2004, Ibanga *et al*., 2017 Thomas *et al*., 2020a. 2020b, 2021, Thomas, 2021). Despite this wide research, earthquake prediction is still a big challenge (Tronin, 2002; Molchanov and Hayakawa, 2008; Freund, 2011). Presently, there is no doubt that multi-precursor analysis is a necessary step to better understand the LAIC mechanism before a large earthquake. Satellite data (Alouette, GEOS 1 and 2, Cosmos 1809, OGO 6, Aureol 3, IK Bulgaria 1300, IK 19 and 24, AE-C, ISIS 2, Topex- Poseidon, DE 2, CHAMP, DEMETER, GPS Satellites,) with free access and wide coverage are available to supplement ground-based data measurements. These data have been used for statistical analyses and an understanding

of the pre-seismic ionospheric variations. Due to the fact that a precursor cannot appear alone before an impending earthquake, multi-precursors analysis is usually taken into account in most studies (Hasbi *et al*., 2009; Revathi *et al*., 2011; Chukwuma *et al*., 2021; Thomas *et al*., 2023). Revathi *et al*. (2011) proposed the comprehensive integration of different earthquake parameters from ground and satellite experiments for better prediction of the event. For instance, Hasbi *et al*. (2009), studied ionospheric and geomagnetic disturbances during the 2005 Sumatran earthquakes using GPS and a magnetometer located near the epicenter. According to their report, ionospheric disturbances were observed at the GPS station 10-24 minutes after the seismic event, while the magnetometer displayed pulsation about 11 minutes after the event.

Ibanga *et al*. (2017) studied unusual ionospheric variations before the strong Auckland Islands, New Zealand, earthquake of September 30th, 2007 using DEMETER and GPS data. From their investigation, both sets of data recorded perturbations 10 days before the earthquake at about the same time. Similarly, Karia *et al*. (2013) analyzed space- and ground-based parameters before an earthquake on December 12, 2009 and observed GPS - TEC enhancement three days prior to the seismic event, while the DEMETER displayed variations in electron density and electron temperature one day before the event. Akpan *et al*. (2019) and Thomas *et al*. (2019) assessed seismo-ionospheric disturbances using Vanuatu and Honshu earthquakes of March 25, 2007 using DEMETER and GPS data According to their submissions, the GPS data analysis showed anomalies two weeks before the EQ under quiet geomagnetic conditions.

In all reported cases, a keen comparison has not been made on which instrument responded faster to the signal. In this paper, we applied these concepts to two earthquakes that occurred in Peru on March 1st, 2019 (M7.0) and August 24th, 2018 (M7.1), using both GPS and magnetometer data, with the aim of finding which of these two instruments responded swiftest to the signals from these events. Details of the studied seismic events are given in Table 1, while figure 1 provides the geographic map of Peru with the epicenters.

Table 1: Details of the studied seismic events

S/N	Magnitude	Date of Event	Time of Event (UTC)	Country	Radius of Preparation Zone (km)	Geo- Coordinates of Epicenter		
						Latitude	Longitude	Focal Depth (km)
1.	7.1	2018- 08-24	09:04:08	Peru	1130	11.036^{0}S	70.828^{0}W	630
2.	7.0	2019 – 03- 01	08:50: 42	Peru	1023	14.713^{0}S	70.155^{0}W	267

2.0 Geomagnetic Data Condition

The Interplanetary Magnetic Field of z – component (IMF-Bz), velocity of the solar wind (Vz), and the geomagnetic parameters of Symmetry–H (SYM–H) and Auroral Electrojet (AE) data were utilized in this study. The IMF-Bz value is perpendicular to the ecliptic and is created by waves and other disturbances in the solar wind. When IMF-Bz turns southward (negative), the direction turns anti-parallel to the

geomagnetic field, which allows the magnetic energy from the sun to penetrate into the earth's atmosphere through the magneto-tail, a process called reconnection. This process consequently leads to the occurrence of a geomagnetic storm. Following the direction of the solar wind (SW) plasma flow, the magnetospheric sheet will move up from the ecliptic plane under a positive SW flow velocity component Vz and down under a negative Vz, irrespective of the sign of the IMF-Bz. The magnetospheric/ring current generated during the ionospheric quiet and disturbed periods was measured by the ground magnetometers. However, the ring current during the geomagnetic storm will be significantly intensified and measured by geomagnetic indices such as the disturbance storm-time index (Dst) and the SYM-H component (Rangarajan, 1989; Wanlissand Showalter, 2006), Unlike the Dst value, which measures in minutes, the SYM-H component has a 1-second temporal resolution, which makes it useful to study short temporal variations during geomagnetic disturbances. Therefore, it is a good proxy for the longitudinally symmetric component of the ring current.

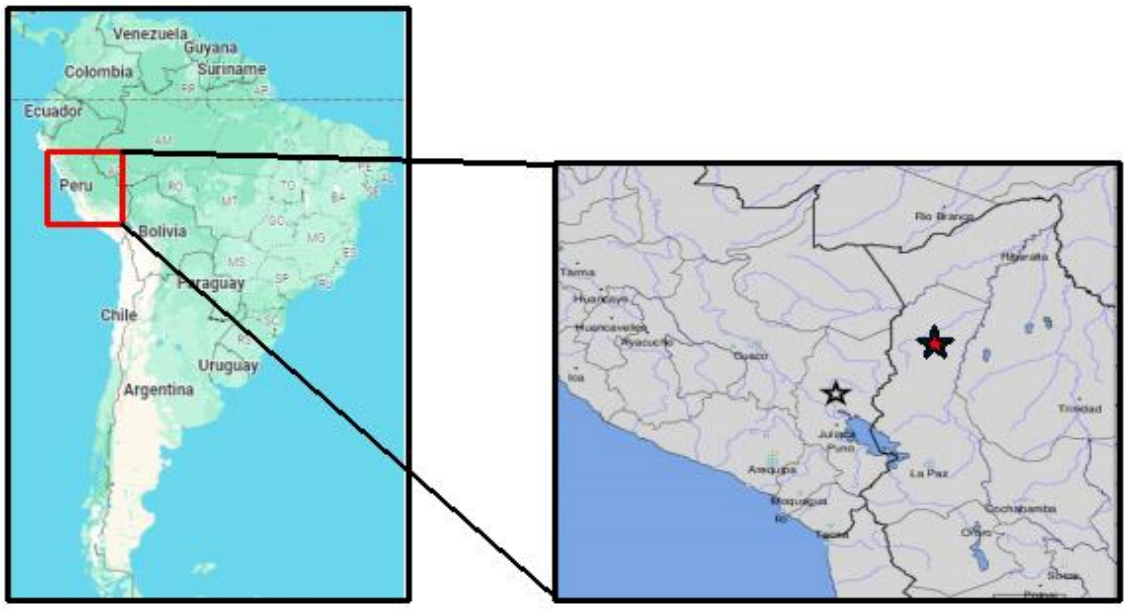

Figure 1: Geographical position of the Peru earthquakes showing the epicenter (the black star shows the epicenter of the M7.0 earthquake of March 1st, 2019, while the red star is the epicenter of the M7.1 earthquake of August 24th, 2018

The AE index is defined as the difference between the AL and AU indices (the largest negative and positive variations of the H component) and characterizes the intensity of the auroral zone currents (auroral electrojet). In quiet times, the value of this index is tens of nT, and during storms and sub-storms it increases to several hundred and more than a thousand nT. During recurrent storms, a high level of background perturbations is observed, along with frequent and intense surges of the AL-index lasting several minutes and a small depth of modulation of the AE-index. The interplanetary magnetic field (IMF) plays a huge role in how the solar wind interacts with Earth's magnetosphere. The AE index is estimated by using 12 observatories magneto-grams of H-component that are uniformly distributed over the

longitude in the northern hemisphere at auroral or sub-auroral latitudes, between 60 ° and 70 °. The geomagnetic data conditions were obtained from the NASA OMNI web service via https://omniweb.gsfc.nasa.gov/.

3.0 Method

The selected earthquakes (Table 1), were individually investigated using both ground - based magnetometer and GPS data within the seismogenic area as opined by Dolbrovosky *et al.* (1979). Both sets of data (magnetometer and GPS) were downloaded within the same duration. For the M7.0 March 1st 2019, Peru EQ, the investigative period was February 26th through March 7th (three days before and six days after). However, a longer period of 17th – 31st August 2018 (seven days prior and after) was opted for the M7.1 August, 24th Peru EQ.

The mean quiet horizontal component field, S_q during the period of the earthquake events was calculated using magnetometer data from selected stations through the International Real-time Magnetic Observatory Network, INTERMAGNET- British Geological Survey (https://imag-data.bgs.ac.uk/GIN_V1/GINForms-2) website. The International Quiet Days (IQDs) and International Disturbed Days (IDDs) were selected from the ftp://ftp.gfz-potsdam.de website, and used to estimate the geomagnetic solar quiet and disturbed days. The one-minute data set of the record of geomagnetic field horizontal component (H), declination component (D) and vertical component (Z) from the stations were estimated and converted to hourly values. Afterward, the variation baseline (Base H) value of each station was computed from the average of the three hours (3 hours) flanking local midnight (01:00LT, 23:00LT, and 24:00 LT) as shown in equation (1) below.

$$Base\ H = \frac{BH_{01} + BH_{23} + BH_{24}}{3}, \qquad (1)$$

where $BH_{01,}$ $BH_{23,}$ and BH_{24} are the hourly values of the H-component at 0100, 2300, and 2400 LT, respectively. To quantify the hourly departure of the H-component that is approximately equal to the hourly solar quiet of the H-component (Sq), the average variation baseline value (Base H) for a particular day from each of the hourly values for that particular day will be subtracted from the hourly value of H-component values from each day (Rabiu *et al*., 2009; Bolaji *et al*., 2013, 2016). The estimation of S_q current for a particular hour or a day in a station can be represented as in equation (2)

$$S_q = H_{compt} - Base\ H \qquad (2)$$

where H_{compt} is the observed H component of the geomagnetic field and Base H is the baseline for that day. The GPS TEC data were calculated by obtaining the slant TEC (STEC) value from the selected GPS receivers used for this study, which were retrieved from the archive of cddis.nasa.gov/archive/gnss/data/website.

According to Fashae *et al*. (2023), the STEC is a relative phase delay along the signal path between the receiver using dual-frequency bands on the 1.57542 GHz (L1) and 1.22760 GHz (L2). The extracted I min STEC data in Receiver Independent Exchange (RINEX) format were polluted with errors such as satellite differential delay, b_S (satellite bias), receiver differential delay, b_R (receiver bias), and receiver inter-channel bias (b_{RX}). Thereafter, the absolute vertical TEC (VTEC) is obtained by subtracting these errors from uncorrected STEC using a mapping function at the ionospheric pierce point (IPP) in relation to the motion of the satellite relative to the receiver of 450 km (Liu et al., 2019; Ma & Maruyama, 2003). These are expressed in equation (3) as:

$$VTEC = \{STEC - [b_R + b_S + b_{RX}]\}/S\,(E) \quad (3)$$

where, S(E), is the obliquity factor with zenith angle, Z, at the ionospheric pierce point (IPP), defined by equation (4).

$$S(E) = \frac{1}{COS(Z)} = \left(\frac{1 - R_E * cos(E)^2}{R_E + h_s}\right)^{-0.5} \quad (4)$$

where R_E is the mean radius of the Earth measured in km and h_S isthe height of the ionosphere from the surface of the Earth taken as 450 km.The TEC unit is the TECU, and one TECU is equal to 10^{16} electrons per square meter.

4.0 Results and Discussions

4.1 M7.0 Peru EQ of March 1st, 2019

Figure 2 panels (a) IMF–Bz (b) Vz (c) SYM–H, and (d) AE indices shows the daily variations of the interplanetary, solar and geomagnetic parameters from 20 February - 7 March 2019, during Peru Earthquake of March 1st, 2019. Before the occurrence of the earthquake on March 2019 the geomagnetic parameters during these periods showed that the geomagnetic activity was quiet. The IMF-Bz was oscillating between the northern and southern hemispheres with minimum value that was less than ~ 10 nT. Vz and SYM-H were seen oscillating around zero with minimal values. There was no data for AE during these periods. During the Earthquake of 01 March 2019 at around ~ 00:00 UT (Figure 2), IMF-Bz was seen oscillating multiple times with no large fluctuations between northward and southward directions Vz fluctuated between ~ 50 km/s and ~ -90 km/s during the same period. Simultaneously, SYM-H was observed to be at the minimum value of ~ -45 nT. The conditions of these parameters indicate no geomagnetic storm occurrence. This fluctuation continued for several days after the earthquake occurrence.

Both magnetometer and GPS data were downloaded from February 26 through March 7th, 2019. Figure 3 presents plots of solar quiet (Sq) in nanotesla against local time (hours) within the study period (a) quiet plot and (b) quiet and disturbed plot as obtained from the magnetometer. As visible in figure 3b, there were differences between the quiet and disturbed plots, heralding variations in the magnetometer. These were observed throughout the investigation period, except on EQ Day.

The difference between quiet and disturbed sq ranged from 5nT to 50 nT. The highest variations occurred on February 28 and March 4, while the least was recorded on the 6th of March. All observed variations were recorded in the morning hours between 7 – 11am. In the same vein, figure 4 shows plots of VTEC (TECU) against Universal Time (hours) from February 26th through March 7th, 2019 (a) quiet plot and (b) quiet and disturbed plot as obtained from the GPS. From figure 4b, two days (26 - 27 February), presented situations with the disturbed plots being above the quiet wiggles. This was recorded in the evening, around 17:00 UTC.

Comparing the responses from the two instruments, it was observed that the magnetometer recorded variations in eight days while the GPS only recorded variations in two days. Both sets of devices simultaneously presented irregularities on February 26 and 27. This is in agreement with the reports of Ibanga et al. (2017), where both DEMETER and GPS detected anomalous variations 10 days before the studied seismic event. However, with respect to the time of response, the magnetometer responded earlier (in the morning between 7-11am) while the GPS detected the earthquake in the evening (17:00 hours). Our results differ slightly from that reported by Hasbi *et al*. (2008) where GPS recorded the signal 10 - 24 minutes before the event while the magnetometer responded 11 minutes before.

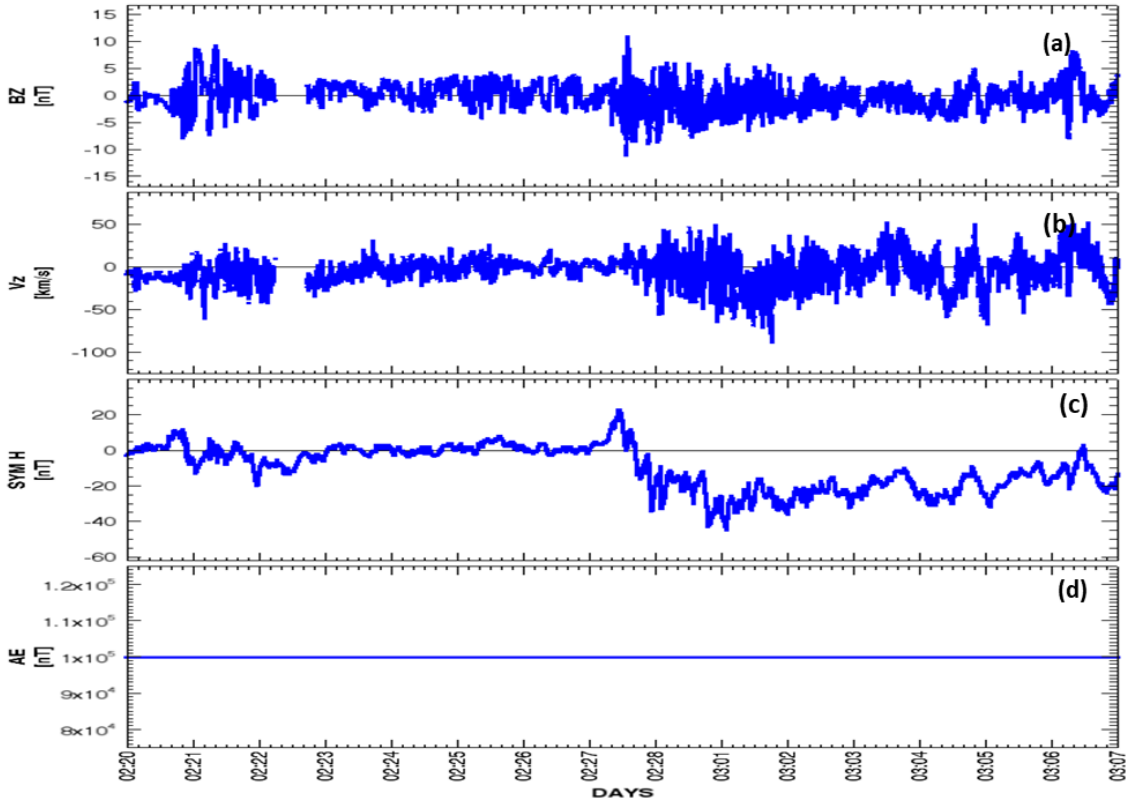

Figure 2: Plots of (a) z–component of the Interplanetary Magnetic Field (IMF–Bz), (b) velocity of the solar wind (SW) Vz, (c) the geomagnetic parameters of symmetry–H (Sym–H) and (d) Auroral Electrojet (AE) indices respectively recorded within the investigation period for the March 1st, 2019 Peru Earthquake

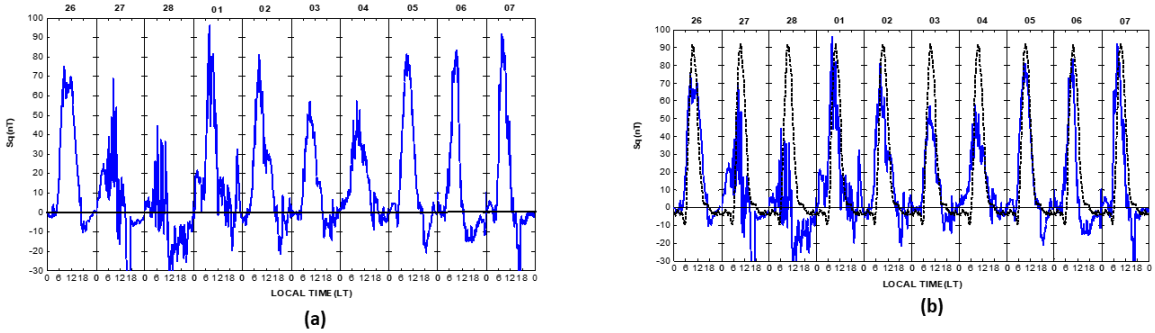

Figure 3: Plots of solar quiet (Sq) in nanotesla against local time (hours) from February 26th through March 7th, 2019 (a) quiet plot and (b) quiet and disturbed plot as obtained from the magnetometer

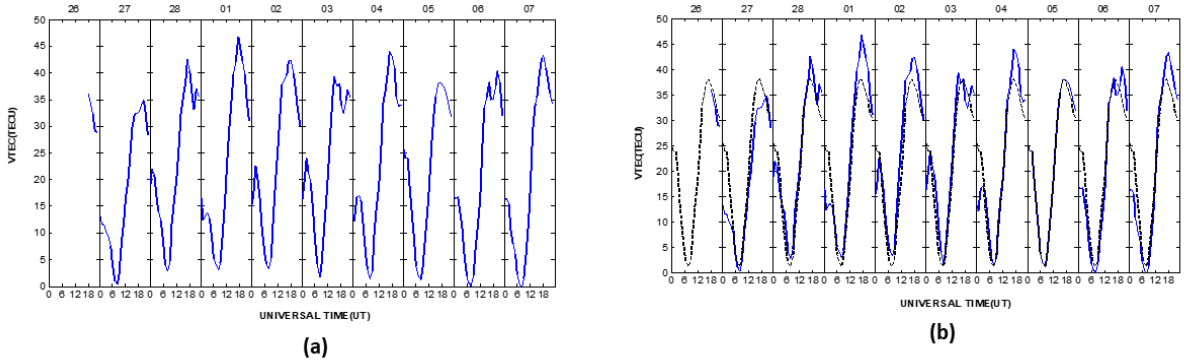

Figure 4: Plots of VTEC (TECU) against Universal time (hours) from February 26th through March 7th, 2019 (a) quiet plot and (b) quiet and disturbed plot as obtained from the GPS

4.2 M7.1 Peru EQ of August 24th, 2018

Both sets of data (magnetometer and GPS) were downloaded from August 17th through August 30th, 2018 to investigate separately the responses of these instruments to the studied EQ. Interplanetary, Solar and geomagnetic data were also acquired within this this time range (Figure 5).During the earthquake of August 24, 2018 (Figure 5), all the geomagnetic parameters were observed to maintain their oscillations around zero. This continued until August 25, 2018 at ~ 16:00 UT, where IMF-Bz, which was exhibiting a northward orientation suddenly, turned southward. This southward orientation continued until it reached a minimum value of ~ -20 nT at ~ 12:00 UT of August 26 2018. At the same time, when IMF-Bz turned southward, SYM-H which was maintaining a mean value of 0 nT started decreasing until it attained the lowest value of ~ -200 nT at ~ 12:00 UT, indicating a severe geomagnetic storm. From ~ 12:00 UT 26 August, SYM-H was observed to begin recovering, and this continued gradually for several days. Vz was observed to not change from its oscillation when IMF-Bz and SYM-H turned, but only started decreasing at ~ 16:00 UT 26 August, reaching a minimum value of ~ -100 km/s. Afterwards, Vz was observed to be oscillating, until it returned to its previous state.

By visible inspection and comparison of Fig. 6a and 6b; from figure 6b, five days (17th, 18th, 20th, 22nd, and 27th August) had disturbed wiggles above the quiet wiggles which were recorded in the morning and mid - morning hours. The rest of the days under study were quiet. The difference between quiet and disturbed sq ranged from 10 nT to 35 nT. The highest variations occurred on 18th August while the least was recorded on the 27th August. All observed variations were recorded in the morning hours between 6 – 11am.

Similarly, Figure 7 shows plots of VTEC (TECU) against Universal Time (hours) from August 17th through 31st, 2018 (a) quiet plot and (b) quiet and disturbed plot as obtained from the GPS. As observed in Figure 7b, the GPS showed no disturbance on the studied days, as the quiet wiggle was above the disturbed wiggle throughout the period. However, Karia et al. (2013), analyzed space- and ground-based parameters before an earthquake observed GPS-TEC enhancement three days, prior to the seismic event, while the DEMETER displayed variations in electron density and electron temperature one day to the event. Comparing the responses from the two instruments, it was observed that only the magnetometer was able to respond to the signals from the EQ whereas the GPS had no response.

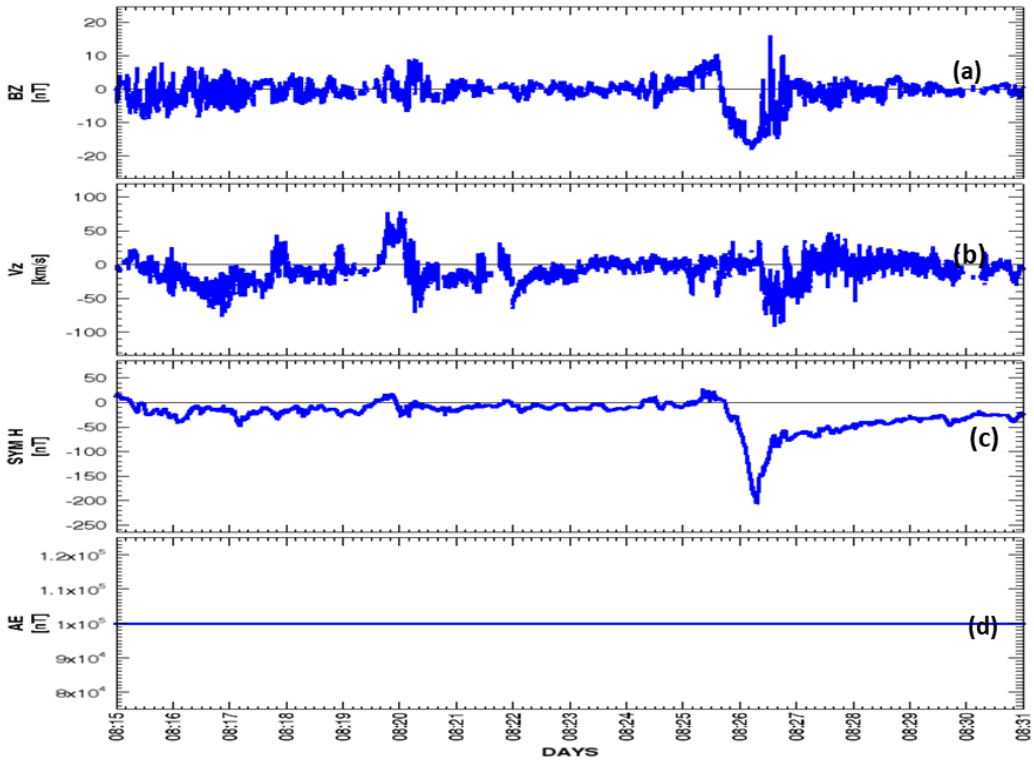

Figure 5: Plots of (a)z–component of the Interplanetary Magnetic Field (IMF–Bz), (b) velocity of the solar wind (SW) Vz, (c) the geomagnetic parameter of symmetry–H (Sym–H) and (d) Auroral Electrojet (AE) indices respectively recorded within the investigation period for the August 24th, 2018 Peru Earthquake.

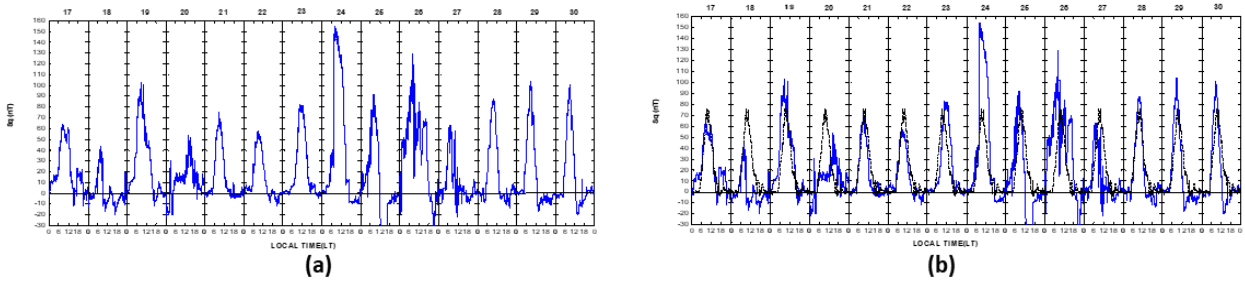

Figure 6: Plots of solar quiet (Sq) in nanotesla against local time (hours) from August 17th through 30th, 2018 (a) quiet plot and (b) quiet and disturbed plot as obtained from the magnetometer

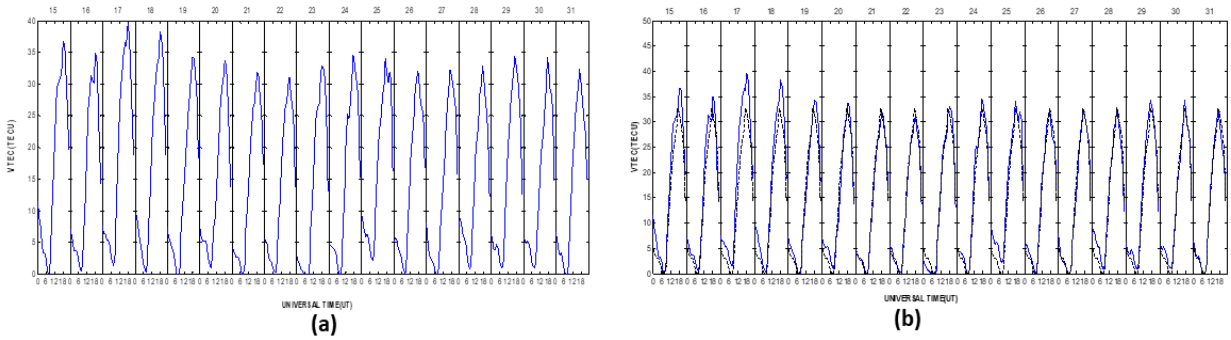

Figure 7: Plots of VTEC (TECU) against Universal time (hours) from August 17th through 31st, 2018 (a) quiet plot and (b) quiet and disturbed plot as obtained from the GPS

5.0 Conclusion

The responses of magnetometer and GPS before two strong seismic events on Peru of March 1st, 2019 and August 24th, 2018 have been well investigated. For the M7.0 March 1st 2019 EQ, an investigation was carried out from 26th February – March 7th 2019 on both devices. It was observed that the magnetometer recorded variations in eight days, while the GPS only responded in two days. The difference between quiet and disturbed sq ranged from 5nT to 50 nT. The highest variations occurred on February 28th and March 4th, while the least was recorded on the 6th of March. All observed variations were recorded in the morning hours between 7 – 11am Both sets of instruments simultaneously presented irregularities on 26 and 27 February. However, with respect to the time of response, the magnetometer responded earlier (in the morning between 7- 11am) while the GPS responded to the signals in the evening (17:00 hours). Also, the M7.1 August 24th 2018 EQ, was investigated between 17th – 30 August using the magnetometer and GPS data. Findings revealed that only the magnetometer was able to respond to the signals from the EQ, whereas the GPS had no response. Hence, in both studied EQ, with different time frames, the magnetometer was found to be more sensitive than the GPS in responding to the variations in the events.

Acknowledgements: The authors appreciate the IGS community for providing the TEC data. We are also very grateful to the USGS and SPEDAS for providing EQ, geomagnetic storm and solar activity data, respectively. The authors are thankful to the Editor in Chief and anonymous reviewers for their comments and suggestions.

Conflict of interest: The authors declare that they have no known competing financial interests or personal relationships that could have appeared to influence the work reported in this paper.

Human and animal rights: This article does not contain studies with human or animal subjects.

References

Akpan, A. E., Ibanga, J. I., George, N. J., Ekanem, A. M. (2019): Assessing Seismo-ionospheric disturbances using Vanuatu and Honshu earthquakes of March 25, 2007, employing Demeter and GPS data. Int J Environ Sci Technol Iran 16(11):7187–7196. https:// doi.org/10.1007/s13762-019-02339-x

Bolaji, O. S., Adimula, I. A., Adeniyi, J. O., Yumoto, K. (2013). Variability of Horizontal Magnetic Field Intensity Over Nigeria During Low Solar Activity. 91–103. https://doi.org/10.1007/s11038-012-9412-0.

Bolaji, O. S., *et al.* (2016). Solar quiet current response in the African sector due to a 2009 sudden stratospheric warming event, J. Geophys. Res. Space Physics, 121, doi: 10.1002/2016JA022857.

Chukwuma, V. U., Adekoya, B. J., Thomas, J. E., Emah, J. B. and Oloruntola, R. F. (2021). On the significance of requisite criteria in detecting pre-earthquake ionospheric precursors: a case study of the Tohoku earthquake of March 11, 2011 Acta Geophysica 69 (4), 1545-1566

Fashae, J. B., Bolaji, O. S., Rabiu, A. B., Ajani, O. O. and Fadiji, J. O. (2023). The Ionospheric Response to the 2013 SSW Event Over the Asian Australian Sector. Journal of Geophysical Research: Space Physics, 128(10), e2023JA031646.

Freund, F. (2011). Pre-earthquake signals: underlying physical processes. J. Asian Earth Sci. 41, 383–400.

Forbes, J. M., Palo, S. E. and Zhang, X. (2000). Variability of the ionosphere; *J. Atmos. Sol.-Terr. Phys.* **62** 685 –693, https://doi.-org/10.1016/S1364-6826(00)00029-8.

Hasbi, A. M., Momani, M. A., Mohd, M. A., Misran, N., Shiokawa, K., Otsuka, Y., Yumoto, K. (2009). Ionospheric and geomagnetic disturbances during the 2005 Sumatran earthquakes Journal of Atmospheric and Solar-Terrestrial Physics Volume 71, Issues 17–18, December 2009, Pages 1992-2005

Hayakawa, M. and Molchanov, O. A. (2002): Seismo-Electromagnetics: Lithosphere-Atmosphere-Ionosphere Coupling. Tok-yo: Terra Scientific Publishing Company, Tokyo.

Ibanga, J. I., Akpan, A. E., George, N. J., Ekanem, A. M. and George, A. M. (2017). Unusual ionospheric variations before the strong Auckland Islands, New Zealand earthquake NRIAG; *J. Astron. Geophys.* **7(1)** 149–154, https://doi.org/-10.1016/j.nrjag.2017.12.007.

Karia, S., Sarkar, S., Pathak, S., Sharma, A. K., Ranganath, H. and Gwal, A. K. (2013). Analysis of space- and ground-based parameters prior to an earthquake on 12 December 2009 https://doi.org/10.1080-/01431161.2013.827341

Kim, V. P. and Hegai, V. V. (1997): On possible changes in the midlatitude upper ionosphere before strong earthquakes. *Journal of Earthquake Prediction Research*, *6*, 275-280.

Liu, Y., Li, Z., Fu, L., Wang, J., and Zhang, C. (2019). Studying the ionospheric responses induced by a geomagnetic storm in September 2017 with multiple observations in America. GPS Solutions, 24(1). doi:10.1007/s10291-019-0916-1.

Liu, J. Y., Chuo, Y. J., Shan, S. J., Tsai, Y. B., Pulinets, S. A. and Yu, S. B. (2004). Pre-earthquake ionospheric anomalies monitored by GPS TEC. *Annals of Geophysics*, *22***,** 1585-1593.

Ma, G., and Maruyama, T. (2003). Derivation of TEC and estimation of instrumental biases from GEONET in Japan. Annales de Geophysique, 21(10), 2083–2093. https://doi.org/10.5194/angeo-21-2083-2003.

Molchanov, O. A. and Hayakawa, M. (2008). *Seismo- electromagnetics and related phenomena: History and latest results*. Toyko: Terra Scientific Publishing Company.

Parrot, M. (1995). Use of satellites to detect seismo-electromagnetic effects, Main phenomenological features of ionospheric precursors of strong earthquakes. *Advances in Space Research, 15*(11), 1337–1347.

Pulinets, S. A., Legen, A. D., Gaivoronskaya, T. V., and Depuev, V.K. (2003). Main phenomenological features of ionospheric precursors of strong earthquakes. *Journal of Atmospheric, Solar and Terrestrial Physics*, *65*, 1337–1347.

Pulinets, S. A. and Boyarchuk, K. A. (2004): *Ionospheric Precursors of Earthquakes*. Berlin:Springer, Verlag Publishers. Germany.

Pulinets, S. A. (1998): Seismic activity as a source of the ionospheric variability. Advances in Space Research 22 (6), 903 – 906.

Rabiu, A. B., Adimula, I. A., Yumoto, K., Adeniyi, J. O. and Maeda, G. (2009). Preliminary results from the magnetic field measurements using Magdas at Ilorin, Nigeria. Earth, Moon and Planets, 104(1–4), 173–179. https://doi.org/10.1007-/s11038-008-9290-7.

Rangarajan, G. (1989). Indices of Geomagnetic Activity. Geomagnetism, Vol. 3, p. 323 – 384

Revathi, R., Brahmanandan, P, Vishnun, T., Uma (2011). Possible prediction of earthquakes by utilizing multi precursor parameters in association with ground and satellite-based remote sensing techniques

Rishbeth, H. and Mendillo, M. (2001). Patterns of ionospheric variability; *J. Atmos. Sol. Terr. Phys.* **63** 1661–1680, https://doi.-org/10.1016/S13646826(01)00036-0.

Thomas, J. E., George, N. J., Ekanem, A. M., Nathaniel, E. U. (2020a). Preliminary investigation of earth tremors using total electron content: a case study in parts of Nigeria. NRIAG J Astronomy Geophysics 9(1):220–225. https://-doi.org/10.1080/20909977.2020.1723866

Thomas, J. E., George, N. J., Ekanem, A. M., Akpan, A. E. (2020b). Ionospheric plasma variations afore the east of Kuril Islands earthquake of 13th January, 2007. Geological Behavior 4(1):42–46. https://doi.org/10.26480/gbr.01 .2020.42.46

Thomas, J. E., Ekanem, A. M., George, N. J., Akpan, A. E. (2021). Electron temperature and ion density perturbations prior to the M6.8 Eastern Honshu, Japan earthquake of July 23, 2008. J Earth Syst Sci. https://doi.org/10.1007/s12040-021-01645-8

Thomas, J. E., Ekanem, A. M., George, N. J., Akpan, A. E. (2023). Ionospheric perturbations: a case study of 2007 five major earthquakes using DEMETER data, Acta Geophysica, 1-12,

Thomas, J. E., George, N. J., Ekanem, A. M., Ekpenyong, N. E. (2019). Ionospheric induced plasma disturbances afore the m7. 9 east-ern Sichuan china earthquake of 12th may, 2008, International Journal of Advanced Geosciences, 7(2), 12-15https://doi.org/10.14419/ijag.v7i2.29980

Thomas, J. E, Ben, U. C. Ekanem, A. M. George, N. .J., Nathaniel, E. U. (2022)**:** Seismo-ionospheric anomalies before M7.2 Haiti earthquake of August 14, 2021, from GPS-TEC Acta Geophysicahttps://doi.org/10.1007/s1160 0-022-00903-7

Thomas, J. E. (2021): Lithosphere-atmosphere - Ionosphere coupling fog Pre-, Co- and post earthquakes: a case study of Northern Mariana, USA earthquake of 31st October 2007. Res J Sci Technol 1(1):37–46

Thomas, J. E., Nathaniel, E. U., George, N. J., Ekanem, A. M., Akpan, S. S. (2024). Statistical analysis of detected ionospheric anomalies with earthquake magnitudes: A case study of the New Zealand earthquakes of March 4, 2021 Results in Earth Sciences 2, 100011

Tronin, A. A. (2002): Atmosphere-lithosphere

Coupling Thermal anomalies on the Earth surface in seismic processes. In: Hayakawa M. and O. A. Molchanov (Eds.), Seismo - Electromagnetics: Lithosphere - Atmosphere -Ionosphere Coupling, *TERRAPUB, Tokyo*, 173-176p.

Wanliss, J. A. and Showalter, K. M. (2006): High resolution global storm index: Dst versus SYM-H. Journal of Geophysical Research https://doi.org/10.1029/2005JA011034